

Lifetime of Positrons in Matter

Yi Gao

Geely University, Chengdu 611430, China

*gift361@163.com

Abstract

Studying positrons in various materials provides valuable information about the fundamental interactions of particles and the properties of matter. For example, medical imaging technique plays critical roles in modern healthcare domain. However, the positron annihilation is the principle behind positron emission tomography (PET). Research on positron lifetimes and annihilation characteristics helps improve the accuracy and resolution of PET scans, contributing to advancements in medical imaging and diagnostics. In this experiment, the source of positron is from Isotope ^{22}Na . Comparing to other general source of positron source such as ^{18}F and ^{11}C , ^{22}Na has three advantages: High Availability, High Positron Yield and Gamma-ray Emission.

Keywords

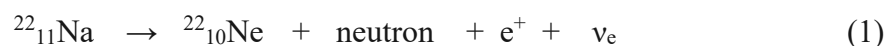
Lifetime of Positrons; PET; Parapositronium; Orthopositronium; ^{22}Na -source; ^{22}Na -spectrum; ^{60}Co -spectrum.

1. Introduction

Positron emission tomography (PET) is critical in medical imaging technique. However, the positron annihilation is the principle behind positron emission tomography (PET). Research on positron lifetimes and annihilation characteristics helps improve the accuracy and resolution of PET scans, contributing to advancements in medical imaging and diagnostics. On the demand of more accurate diagnoses in fields such as oncology, neurology, and cardiology, improving the sensitivity and resolution of PET scanners is absolutely necessary and urgent. Understanding the lifetime of positrons in PET is crucial to push the boundary of the performance of PET.

Generally, in lab, there are multiple options for the source of positrons, such as ^{18}F and ^{11}C . Nevertheless, this experiment applies Isotope ^{22}Na to offer positrons. Comparing to the formers, ^{22}Na has three advantages: High Availability, High Positron Yield and Gamma-ray Emission.

^{22}Na undergoes beta-plus decay, a process in which a proton is converted into a neutron with the emission of a positron and a neutrino. The decay equation is:



To verify the precision and accuracy of measurement, this experiment analyze the lifetime of positrons in both in aluminum and PET. The measurement can then be terminated upon detection of a photon created by positron annihilation and therefore at the end of its lifetime. In addition to the measurement of lifetime-spectra, the ratio of parapositronium and orthopositronium can be determined.

2. Set-up and Execution of the Experiment

To measure the lifetimes, it is necessary to detect the particles of the radioactive decay. Two opposite detectors made from scintillator with one Photo Multiplier Tube (PMT) powered by 1900 V are used. The set-up consists of two circuits: *Fast Circuit* measures the time difference between the *Start* and *Stop* signals, while *Slow Circuit* which filters the signals for specific energies to distinguish the particles and trigger a data acquisition if the desired particle combination is detected, see Fig. 1.

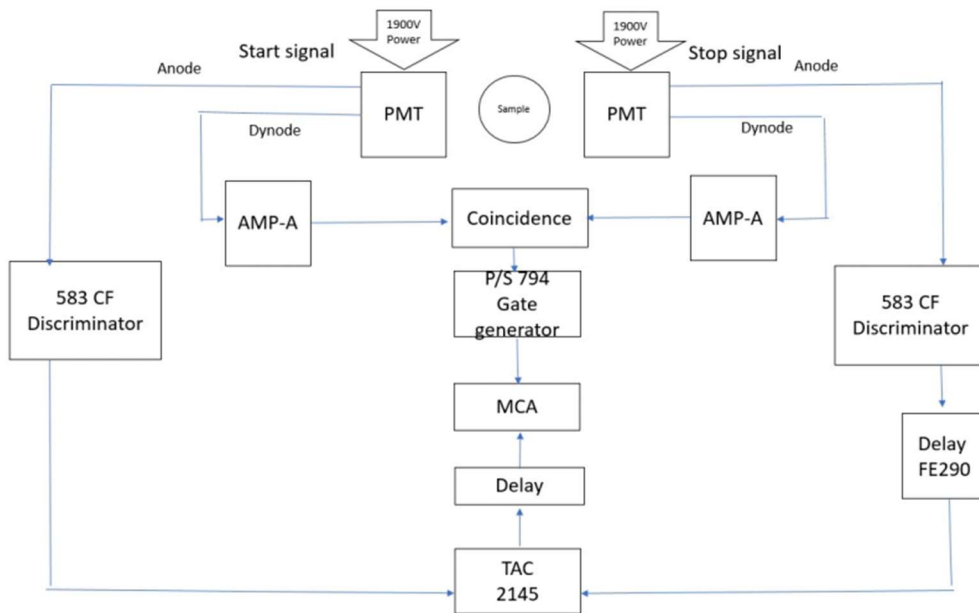


Fig.1 Electronic Block diagram of the general set-up

The anode-signals are sent into CFDs (Ortec 583 Constant-Fraction Discriminators) in CF mode. The anode-pulse has a typical amplitude of about -1.5 V which lays in the CFDs' accepted input range. It has a rise time of about 3 ns and a width of approximately 15 ns. Both of the CFDs use a 0.5 ns delay cable. The Walk potentiometer is adjusted to ensure the triggering always happens at the same time relative to the pulse's course. The *Stop* signal is delayed by 24 ns with an SEN FE290 delay unit. The *Start* and *Stop* signals meet in the TAC (Time- to-Amplitude Converter Canberra 2145) as they are connected to its *Start*- and *Stop*-input respectively. The TAC converts the time difference into a proportional pulse height. To make sure the TAC covers the whole spectrum it is set to a 50 ns time range with the Multiplier set to 1. A spectrum of the pulse heights is then recorded using a Multichannel Analyzer (Canberra Multiport II). The gate to trigger the data taking of the MCA is delivered by the *Slow Circuit* if particles of the correct energies are detected. To ensure the TAC signal lays in the gate, it is delayed by 3 μ s with a delay amplifier (Canberra 1457) set to 10 V range. The PMTs' dynode outputs are connected to AMP-As (amplifier analyzer NE 4630). The thresholds and windows of the AMP-As are tuned to filter for the desired energies. Both are set to a gain of 300 and a time constant of 0.3 μ s. For the *Start* signal, the threshold is set to 1.46 in integral mode to filter for particles with higher energy to detect the 1.28 MeV photon. For the *Stop* signal, the AMP-A is set to differential mode with a threshold of 0.1 and a window of 1.9 to detect only the energy in the range of the annihilation photons. The selected signals are coupled by the internal coincidence of the AMP-A with a time window of about 1 μ s. The coincidence output is connected to a gate generator (PS 794) that creates a gate with 4.5 μ s. The duration makes sure the MCA measures the whole signal from the TAC. Once the MCA receives a gate from the *Slow Circuit*, the pulse of *Fast Circuit* is recorded and sorted into bins (channels) according to their amplitude. It produces a histogram of pulse height spectrum.

3. Time Calibration

In order to convert the pulse-height-spectrum recorded with the MCA to a lifetime spectrum, a time calibration is needed. As the pulse height is determined by the time difference between the Start and Stop signal given into the TAC, it is necessary to artificially create those signals with a known time duration between them to obtain points that can be used for calibration. For this purpose a pulse generator is used to create the signals. One of the pulse generator's outputs is connected with the CFD used for the start-signal while another output is connected to the CFD used for the stop signal. At a frequency of 500Hz, pulses are created while a delay between the two outputs can be freely chosen. Starting with 0ns, the delay between the two outputs is increased in steps of 1ns. For each step, the height-spectra of the resulting TAC-pulses is recorded for at least one minute.

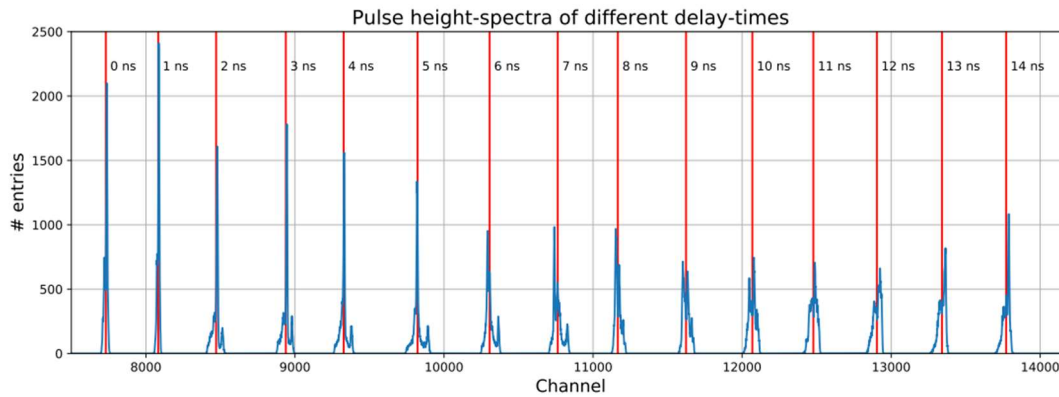


Fig.2 Pulse height-spectra of different delay times

In Fig.2, it becomes clear that the distributions spread over around 100 channels, with many distributions showing second peaks. The centroid method is used to determine the channel number i corresponding to each time difference (delay of i ns), where k is the channel number and $N_{i,k}$ the corresponding number of entries. where k is the channel number and $N_{i,k}$ the corresponding number of entries:

$$n_i = \sum_{k=1}^N \left(k \cdot \frac{N_{i,k}}{\sum N_{i,k}} \right) \quad (2)$$

According to the pulse generator's manual, the deviation u_{td} of the set delay time t_d is calculated using:

$$u_{td} = 500\text{ps} + 25 \cdot 10^{-6} \cdot t_d \quad (3)$$

Using the values and uncertainty of the peak positions obtained using the centroid method and the set delay times with uncertainties according to Equation (3), a linear regression is programmed and performed using Python. The result of the fit is presented in Fig.3. The obtained function:

$$t(n) = 0.0028 \text{ ns} \cdot n - 17.42 \text{ ns} \quad (4)$$

contains the time-width of one channel Δt_C as the slope of the curve.

$$\Delta t_C = (2.28 \mp 0.02) \text{ ps} \tag{5}$$

This calibration will be used for every further conversion from channel numbers to time differences.

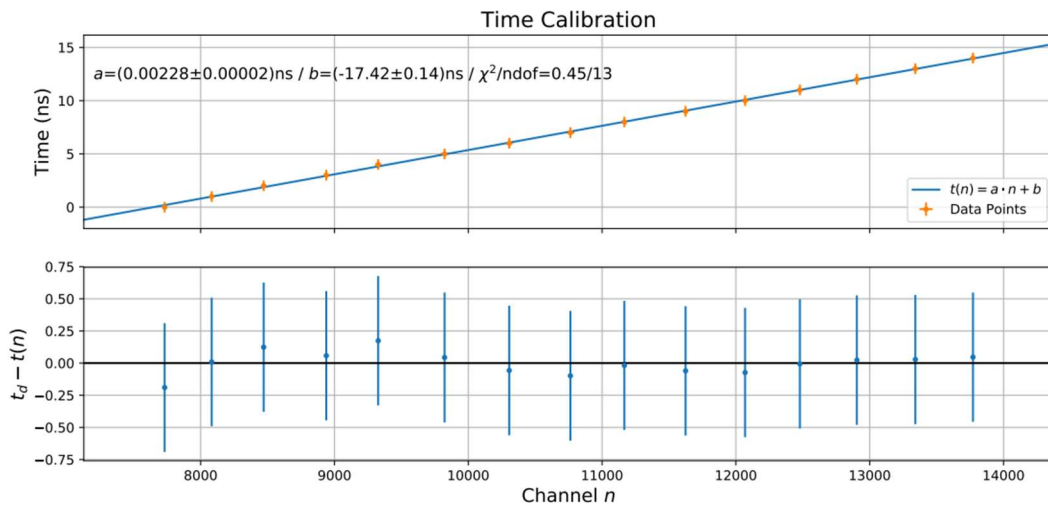


Fig.3 Linear regression of the time calibration

The width of the 0 ns peak corresponds to the pure electric time resolution Δt_{PE} of the setup. Using the uncertainty $\sigma_{n0} = 10.07$ obtained using the centroid method, the time resolution is calculated by multiplication with the time width of one channel Δt_C .

$$\Delta t_{PE} = (22.9 \pm 0.1) \text{ ps}$$

4. Time Resolution using ^{60}Co

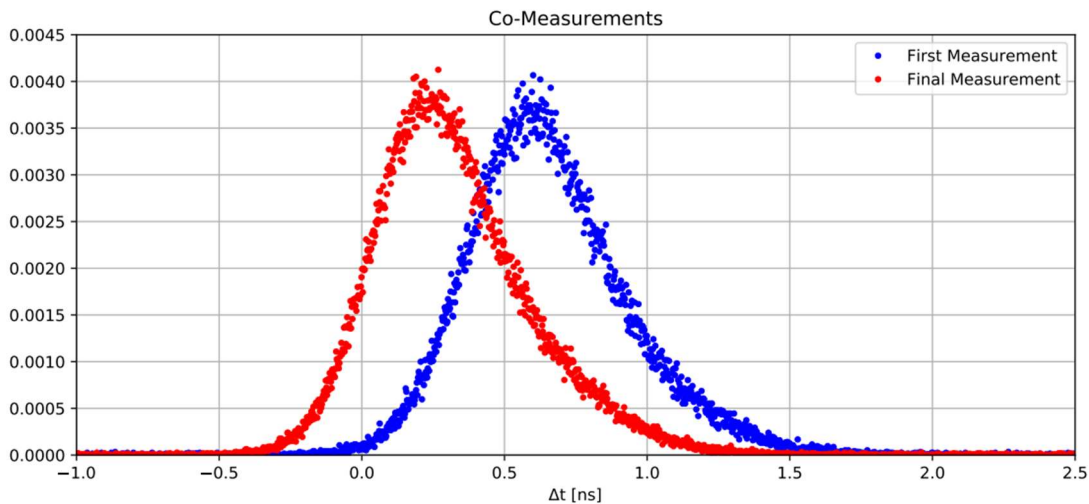


Fig. 4 Comparison of the two cobaltments

The pure electric time resolution is not the time resolution of the full setup as additional components are present. To determine the time resolution curve a ^{60}Co source is used, as it emits two almost

simultaneous photons with energies of more than 1 MeV. Therefore, the amplifier analyzer observing the *stop*-signal is set to Integral mode. The measurement (measured for about 1 h) is done before the ²²Na-spectra are recorded and repeated once afterwards (measured for about 1.5 h). The delay of 24 ns shifts the whole measurement to higher channels, which enables the use of the lower channels to determine the background of the measurements. The mean of the entries in the channels 500-6500 is calculated and then subtracted for each measurement. The two normalized ⁶⁰Co- measurements after the background-subtraction and with the channels converted to the corresponding time differences are plotted in Figure 4. A clear shift is visible.

Neglecting negative counts resulting after the background subtraction, the calculation yields:

Table 1. Mean Channel Positions of Cobalt measurements

Measurement	$n \mp \sigma_n$
Co First	7950 \mp 4
Co Final	7813 \mp 3

The error caused by the background subtraction (the backgrounds are 1.275 \mp 0.013 (first) and 1.781 \mp 0.013 (final)) can be neglected. The results can be found in Table 2:

Table 2. Mean time positions of Cobalt measurements

Measurement	$t \mp \sigma$
Co First	(0.69 \mp 0.17)ns
Co Final	(0.38 \mp 0.17)ns

The ²²Na spectrum in PET used in the analysis is in fact taken after the second measurement with ⁶⁰Co because of a failure of the first measurement (possibly due to a faulty delay module).

Both curves in Fig.4 measure the spectrum of the same source with an identical setup and should therefore show identical results. This is not the case, as a clear shift of the peak position (of about 0.3 ns) is present. Because of this shift happening without any change of the setup, it becomes evident that the setup is of low stability. An explanation for this shift might be a change in temperature, lack of precision of modules used or a possibly malfunctioning delay module, as baseline-jumps in its output can be observed in the oscilloscope for a short time after changing the delay time.

The experimental time resolution Δt_E can be determined by calculating the width at half maximum. Because there is a shift between the two Cobalt measurements, only one is suitable for further analysis (the final one). Therefore, the experimental time resolution for the following analysis is (527 \mp 5)ps.

5. Measurement Using ²²Na in Matter

5.1 Measurement Using ²²Na in Aluminum

In order to measure the lifetime of positrons in metal, a ²²Na-source embedded in aluminum is placed in the setup. In this case, the two CFDs are used to distinguish the start photon (1.28 MeV) and the stop photon (p+ annihilation). The spectrum is recorded for about 4 h. The raw data can be found in the appendix. Figure 6 shows the spectrum after background subtraction (as described above) and normalization together with the two cobalt-measurements.

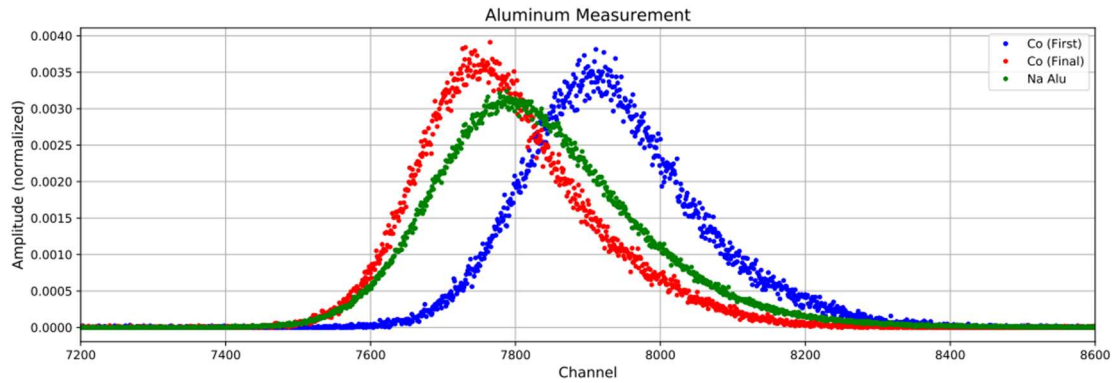


Fig.5 Aluminum measurement together with the cobalt curve

The maximum of the ^{22}Na -spectrum should be shifted to the right compared to and located on the ^{60}Co -spectrum which is the case for the final ^{60}Co -measurement. As the ^{22}Na -spectrum is shifted to the left compared to the first ^{60}Co -measurement, it is obviously not compatible as the shift would imply a negative value for the positron lifetime which is unphysical. To determine the lifetime of the positrons the centroid method is used as described in the manual using python. The lifetime of positron in Aluminum is:

$$\tau = (68 \mp 7) \text{ps}$$

5.2 Measurement Using ^{22}Na in PET

In contrast to the measurement with aluminum, positrons engage in positronium formation in PET. Those processes result in different lifetimes that are connected to the positronium-lifetimes. Like with the aluminum measurement, a ^{22}Na source is used, this time embedded in PET. It is placed in the set-up and measured for about 15.5 h. The raw measurement can be seen in the appendix, the spectra after background subtraction and normalization together with the ^{60}Co measurements are plotted in Fig.6.

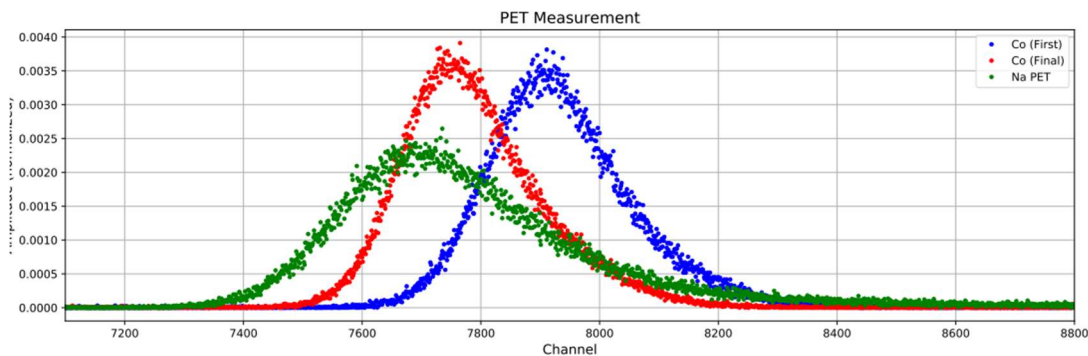


Fig.6 PET measurement together with the cobalt curves

Fig.6 shows the spectrum in PET is broadened compared to the ^{60}Co -spectra. This is due to the higher lifetimes. Additionally, the instability of the set-up is again visible, by the fact that the spectrum is located on the left of both time resolution curves, which would imply a negative lifetime but is caused by the whole x-axis apparently shifting to the left over time.

5.2.1 Positron Lifetime

Due to the incompatibility of the recorded spectrum with the ^{60}Co -data and the larger expected lifetimes, the approximated tail method is used to determine the lifetimes of para- and orthopositronium. The lifetime τ can be extracted from a measurement $F(t)$ via:

$$\frac{d}{dt} \ln F(t) \approx -1/\tau \tag{6}$$

Therefore, the logarithm of every bin content after background subtraction and normalization is calculated and a linear regression is performed on two different slopes of the tail. The plot of the normalized measurements' logarithm with the two linear parts drawn in can be seen in Fig.7. Bins in the area $t > 1.3$ ns are rebinned, where four bins are put together as one new bin.

The linear parts used for analysis are marked. The data is re-binned into groups of for times larger than 1.3 ns.

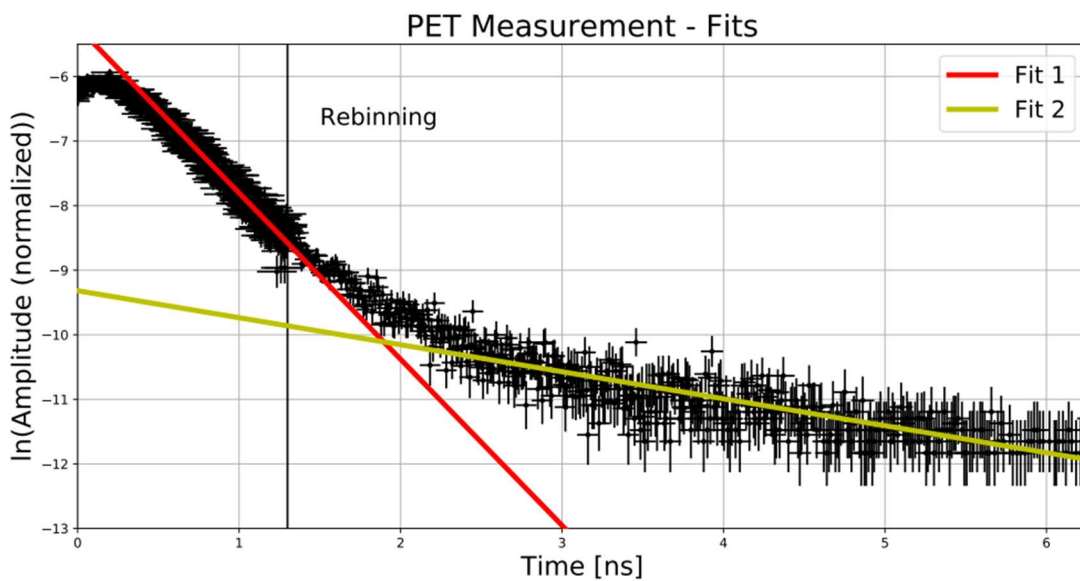
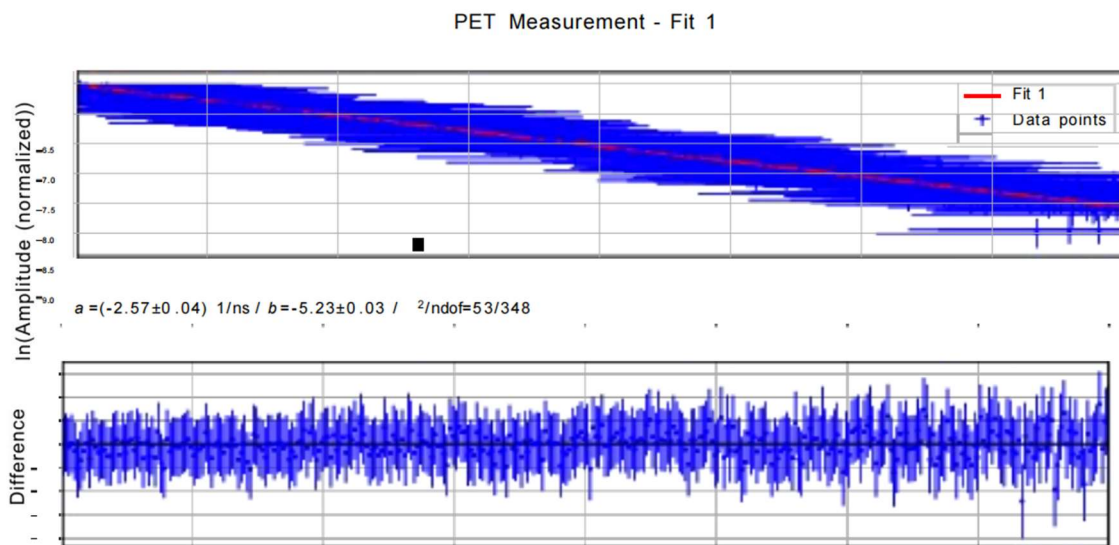


Fig.7 Logarithm of the normalized spectrum

The subtracted background is 0.038 ± 0.003 and its uncertainty is neglected.



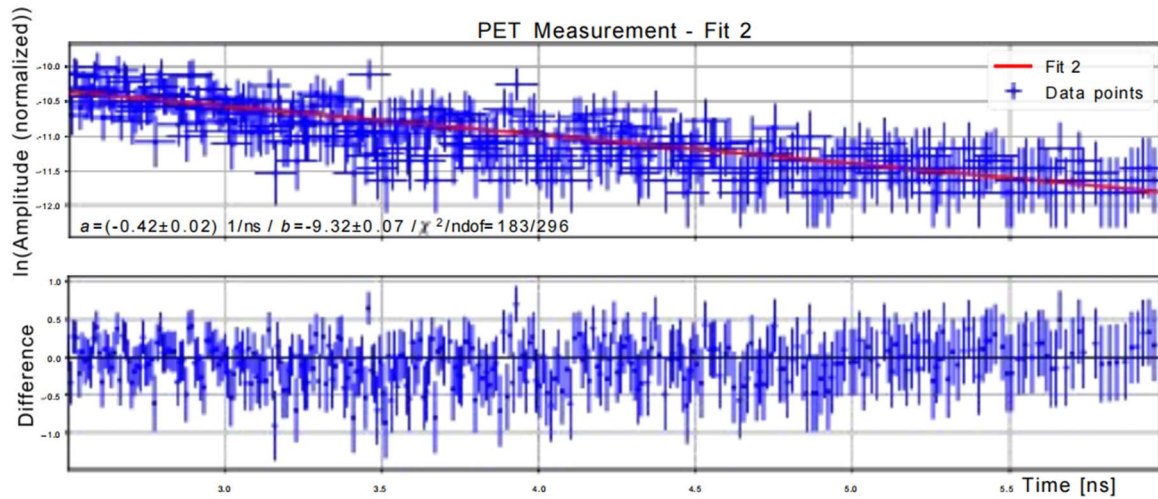


Fig.8 Fit of the first and second linear part

The subtracted background is 0.038 ∓ 0.003 and its uncertainty is neglected. The linear fits are performed using python and are presented in Fig.8. The general trend of both sections is well described with a linear fit. The $\chi^2 / \text{ndof} < 1$ might indicate overestimated uncertainties. As explained, the relevant parameter of the fit is the slope, as it enables the approximate calculation of the lifetime using:

$$\tau \approx -1/a \tag{7}$$

The uncertainty of τ is then:

$$\sigma_\tau = \sigma_a / a^2 \tag{8}$$

The slopes and the calculation lifetime results are presented in Table 3.

Table 3. Result of the PET measurement

	Fit 1	Fit2
a	$(-2.57 \mp 0.03) \text{ 1/ns}$	$(-0.42 \mp 0.02) \text{ 1/ns}$
τ	$(0.388 \mp 0.005)\text{ns}$	$(2.4 \mp 0.1)\text{ns}$

The shorter lifetime (Fit 1) can be associated with the lifetime of parapositronium while the longer lifetime (Fit 2) corresponds to converted orthopositronium:

$$\begin{aligned} \tau_{\text{Para}} &= (0.388 \mp 0.005)\text{ns} \\ \tau_{\text{Ortho}} &= (2.39 \mp 0.10)\text{ns} \end{aligned}$$

5.2.2 Ratio of Parapositronium and Converted Orthopositronium

The fit from Fig.9 is used in an attempt to recreate the underlying decays of the spectrum and calculate the ration between parapositroium and orthopositronium.

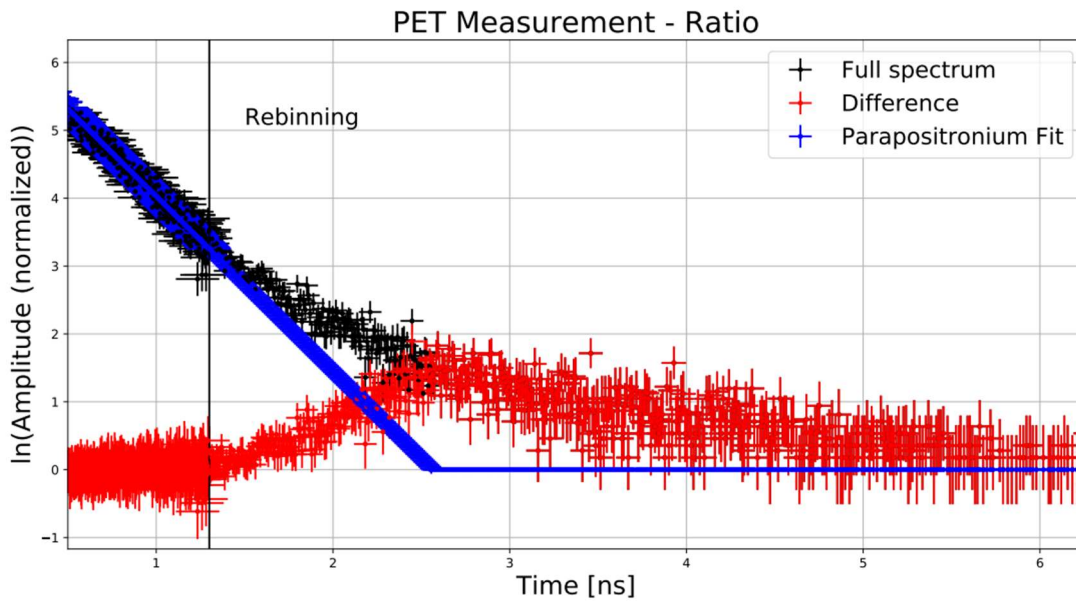


Fig.9 Reconstruction of the parts of the spectrum

To determine the ratio, the logarithm is reversed by applying the exponential function. The sum of all entries of the parapositronium curve S_P is calculated as well as the sum of all entries of the orthopositronium curve S_O . The ratio R between converted orthopositronium and parapositronium can then be obtained:

$$R = S_O / S_P \tag{9}$$

For every step of the calculation Gaussian error propagation was performed to calculate the uncertainty of the ratio, the result is:

$$R = (1.90 \pm 0.05)$$

6. Results and Discussion

The results of all measurements are collected in Table 4.

Table 4. Results of the positron lifetime measurements

Positron lifetime in aluminum	$(68 \pm 7)\text{ns}$
Parapositronium formation lifetime in PET	$(0.388 \pm 0.005)\text{ns}$
Orthopositronium formation lifetime in PET	$(2.4 \pm 0.1)\text{ns}$
Ratio of para- and converted orthopositronium in PET	$(1.90 \pm 0.05)\text{ns}$

As explained in the manual, the expected lifetime of positrons in aluminum is of a few picoseconds but no explicit value is given. The obtained result of $(68 \pm 7)\text{ps}$ might be in the right order of magnitude but is probably too large. This might be explained by the left shift observed during the course of the experiment or a non sufficient time resolution, as the experimental time resolution is about 500ps large. The lifetime of Parapositronium was calculated in preparation for the experiment to be 0.1254 ns . As the positronium forms after the stopping of the positron which takes about 0.22ps

(see manual), a time difference between the start and stop signal of about 0.345ps is expected. The obtained value of (0.388 ± 0.005) ns is of the same order of magnitude. Due to the small uncertainty on the measured time, it is over 8 sigmas away from the expected value. This might be due to the fact that positrons take a small duration of time after stopping to form positron. Additionally, possible sources of uncertainties might have been underestimated and the setting of the setup might have been not optimal.

7. Conclusion

The lifetime of the positron with the formation of orthopositronium with a value of (2.4 ± 0.1) ns is much smaller than the lifetime of orthopositronium alone that was calculated to be 138.7 ns. This is to be expected as the orthopositronium can convert into parapositronium and then decay with the parapositronium's lifetime. The ratio between parapositronium and converted orthopositronium has been computed to be $(1.90 \pm 0.05)\%$ (orthopara). This means that only very few orthopositronium convert into parapositronium fast enough to be measured in the set range.

The results are of the expected order magnitude. With a high instability of the set-up was observed which caused the recorded spectra to shift to left. It is unclear what caused this behaviour but a defective delay module might be the reason.

References

- [1] David Griffiths: Introduction to elementary particles (WILEY-VCH Verlag GmbH & Co. KGaA, America 2005), (In English).
- [2] K Kotera , T Saito ,T Yamanaka : Measurement of positron lifetime to probe the mixed molecular states of liquid water, Physics Letters A, Vol. 345(2005), p. 184-190.
- [3] A. Ingram, R. Golovchak: Compositional dependences of average positron lifetime in binary As-S/Se glasses, Physica B: Condensed Matter, Vol.407(2012),p. 652-655.
- [4] Dryzek: Remarks on a source contribution in positron lifetime measurements, Beam Interactions with Materials and Atoms, Vol.521(2022), p.1-6.
- [5] Steven D. Bass, Sebastiano Mariazzi, Pawel Moskal: Positronium physics and biomedical applications, Rev. Mod. Phys. Vol.95 (2023), p.95-103.